



Universidad Autónoma
de Madrid

Biblos-e Archivo
Repositorio Institucional UAM

Repositorio Institucional de la Universidad Autónoma de Madrid

<https://repositorio.uam.es>

Esta es la **versión de autor** del artículo publicado en:
This is an **author produced version** of a paper published in:

Journal of Physical Chemistry B 122.2 (2018): 534-542

DOI: <https://doi.org/10.1021/acs.jpcc.7b04227>

Copyright: © 2017 American Chemical Society

El acceso a la versión del editor puede requerir la suscripción del recurso
Access to the published version may require subscription

Adsorption geometry and energy level alignment at the PTCDA/TiO₂(110) interface

Sylvie Rangan,^{1,*} Charles Ruggieri,¹ Robert Bartynski,¹ José Ignacio Martínez,² Fernando
Flores,^{3*} and José Ortega³

¹ Dept. Physics and Astronomy, and Laboratory for Surface Modification, Rutgers, The State
University of New Jersey, Piscataway, NJ 08854-8019 (USA)

² Dept. Surfaces, Coatings and Molecular Astrophysics, Institute of Materials Science of
Madrid (ICMM-CSIC), Sor Juana Inés de la Cruz 3, ES-28049 Madrid (Spain)

³ Dept. Física Teórica de la Materia Condensada and Condensed Matter Physics Center
(IFIMAC), Universidad Autónoma de Madrid, ES-28049 Madrid (Spain)

ABSTRACT

The adsorption geometry and energy alignment at the PTCDA/TiO₂(110) interface are investigated using a combination of experimental and theoretical approaches. The energy alignment is determined experimentally from the occupied and unoccupied states electronic structure measured using x-ray and UV photoemission and inverse photoemission, respectively. Two possible adsorption geometries compatible with previous studies, a flat geometry and a tilted geometry, were explored using DFT techniques, in order to obtain theoretical STM images and energy alignment at the interface. Both STM images simulation and resulting energy alignment point to a tilted geometry for PTCDA on TiO₂(110).

I. Introduction

Owing to their extended π systems, polyaromatic molecules have been candidates of choice as organic semiconductor materials in a wide range of applications from organic electronics to light harvesting devices.¹⁻⁵ Although the intrinsic bulk properties of the organic material such as molecular packing and electronic structure determine, for example, energy absorption and carrier propagation mechanisms, in many applications there are crucial effects imposed by the properties of the interface between the organic semiconductor and another organic material, a metal or an oxide surface.¹⁻⁵

A large body of work addresses the properties of organic-organic and organic-metal interfaces.⁶⁻⁸ In contrast, prediction of the properties of organic-oxide interfaces is still challenging. Recent work has emphasized the importance of the electron chemical potential equilibration between the oxide Fermi level and the organic ionization energy to describe the energy alignment of organic molecular levels with respect to the band edges of oxides.⁹ However, effects such as electron charge transfer upon molecular adsorption with possible space charge layer formation in the oxide,¹⁰⁻¹¹ as well as the very nature of the chemical interaction of the organic on the oxide surface are important considerations in any attempt to fully understand such interfaces.^{3, 10, 12-13}

PTCDA (Perylene-3,4,9,10-tetra-carboxylic dianhydride) is one of a number of polyaromatic organic materials that have been viewed as prototypical molecules for the studies of heterointerfaces.^{1, 14} It is particularly attractive owing to its strong optical absorption properties in the visible range and to its molecular packing that enables π/π overlap resulting in remarkable electronic properties.^{1, 15-16} The adsorption properties of PTCDA have been studied for a wide range of surfaces, from metals to oxides.^{14, 17-18} On most surfaces, and in particular on noble metals, PTCDA was found to adsorb in a flat geometry and to form ordered monolayers.¹⁴ On TiO₂(110), however, contradictory accounts for the surface geometry have been reported. Early scanning tunneling microscopy (STM) studies have concluded that the molecule adopts a flat lying geometry when adsorbed on this surface¹⁹⁻²⁰. More recently, several spectroscopic studies using X-ray photoelectron spectroscopy (XPS) and near edge X-ray absorption fine structure (NEXAFS) spectroscopies seem to indicate that the PTCDA molecules adsorb in a tilted geometry, with the plane of the molecule making an angle of about 50° with respect to the surface normal.²¹⁻²² Studies of a closely related molecule PTCDI (perylene tetra carboxylic diimide, a parent molecule to PTCDA in which the central oxygen of the carboxylic dianhydride group is replaced by a N-H group) adsorbed on TiO₂(110) also points to a tilted adsorption mode, and ab-initio calculations seem to favor a geometry in which the longest edge of the molecule is interacting with the surface.²³ Similar observations have been made for other

conjugated polyaromatic molecules such as perylene²⁴ and pentacene²⁵ adsorbed on the TiO₂(110) surface. In addition to this controversy, reports of the energy alignment properties at the PTCDA/TiO₂(110) interface are scarce^{22, 26} and typically only include measurements of the occupied energy states using photoemission spectroscopy. As a result, one is in the undesirable position of using quantities from significantly different measurement techniques, such as optical gaps, and appending them to photoemission data sets in order to build a complete energy diagram of the interface electronic structure.

The aim of our work is to determine and understand the energy alignment of the adsorbate occupied and unoccupied molecular levels and the substrate valence and conduction band edges for the PTCDA/TiO₂(110) system using a combination of experimental (XPS, ultraviolet photoemission spectroscopy (UPS) and inverse photoemission spectroscopy (IPS)) and theoretical techniques (density functional theory (DFT) and theoretical STM). In particular, we have considered the two main adsorption geometries proposed in the literature, one flat and one tilted, and compared the results of state of the art DFT calculations to new electronic spectroscopic measurements and published STM images, so as to address both the energy level alignment at the interface and the interpretation of the STM images. We conclude that only a tilted geometry can reconcile both the STM images found in the literature and the measured energy level alignment, found extremely sensitive to the adsorption geometry of the PTCDA molecules.

II. Methods

Surface preparation

The rutile TiO₂(110) sample was a commercially produced single-crystal from MTI corporation, cut to within 0.5° of the (110) plane. The surface was degassed and prepared in an ultrahigh vacuum using several cycles of 1 keV Ar⁺ ion sputtering (while maintaining a maximum sample current of 2 μA) and annealing in UHV at 600°C. The cleanliness of the surface was checked using XPS, and the surface termination was assessed by low energy electron diffraction (LEED).

Perylene-3,4,9,10-tetra-carboxylic dianhydride (PTCDA) molecules [Aldrich 97% purity] were deposited by way of sublimation in the same UHV environment using a thoroughly degassed Knudsen cell held at 380°C. The deposition rate was measured using a quartz crystal monitor.

Spectroscopic methods

XPS, UPS, and IPS measurements were performed in a single UHV experimental system described elsewhere.²⁷ In UPS and XPS, the kinetic energy distribution of electrons ejected by excitation from monoenergetic photons reflects the density of occupied states in the system. In IPS, a monoenergetic beam of electrons is directed to the sample and a small fraction undergoes

optical decay emitting photons. The resulting photon energy distribution reflects the density of unoccupied states in a manner that is highly complementary to UPS. Core levels were probed using X-ray photoemission spectroscopy excited by non-monochromatized Al K α radiation, and the valence band electronic states were examined using He II (40.8 eV) excited ultraviolet photoemission spectroscopy. In both cases, electron energy distributions were measured using a cylindrical mirror analyzer.

The conduction band spectra were obtained from inverse photoemission spectroscopy performed using a grating spectrometer with a primary electron energy of 20.3 eV. The overall energy resolution for the UPS and IPS spectra is estimated to be better than 0.3 and 0.6 eV, respectively. The energy scales of the UPS and IPS spectra were calibrated using the measured position of the Fermi level of a gold sample in contact with the oxide sample. For all spectra, the Fermi level is the zero of energy, occupied electronic states are assigned negative energy and unoccupied states positive energy.

For both the clean and PTCDA-covered surfaces, the secondary electron cutoff has been measured on biased samples using a He I radiation (21.1 eV) so as to determine the electron affinity, given by $EA = h\nu - W - E_{gap}$, where $h\nu$ is the photon source energy, W the total width of the spectra, and E_{gap} is the experimentally measured gap of the oxide surface (i.e., the energy difference between the valence band maximum (VBM) measured by UPS and the conduction band minimum (CBM) measured by IPS) or the molecular gap (i.e., the energy difference between the centroids of the highest occupied molecular orbital (HOMO) measured by UPS and the lowest unoccupied molecular orbital (LUMO) centroid measured by IPS).

Theoretical methods

Computational details

For the *ab initio* structural optimization, electronic structure and theoretical STM-imaging simulations of the different PTCDA/TiO₂(110) configurations analyzed in this paper, Density Functional Theory (DFT) was used effectively combining the plane-wave and localized-basis-set schemes as implemented in the QUANTUM ESPRESSO simulation package²⁸ – used for the determination of the complex interface atomic geometries –, and in the FIREBALL simulation code²⁹⁻³¹ – used to analyse the interface electronic properties after introducing appropriate correlation effects on the electronic levels of the organic molecule (see below), as well as for the simulation of the theoretical STM images. For the plane-wave code QUANTUM ESPRESSO,²⁸ one-electron wave-functions were expanded in a basis of plane-waves, with energy cut-offs of 400 and 500 eV for the kinetic energy and for the electronic density, respectively, which have been adjusted to achieve sufficient accuracy in the total energy. The exchange-correlation (XC) effects have been accounted for by using the revised version of the generalized gradient corrected approximation (GGA) of Perdew, Burke, and Ernzerhof (rPBE),³² and norm-conserving scalar-relativistic pseudopotentials have been considered to model the ion-electron interaction. In the calculations, the Brillouin zones (BZ) were sampled by means of optimal Monkhorst-Pack grids³³ guaranteeing a full convergence in energy and electronic density. A perturbative van der Waals (vdW) correction was used to check the reliability of all the adsorbed

adlayer configurations. For this purpose, we have used an empirical efficient vdW R^{-6} correction to add dispersive forces to conventional density functional (DFT+D).³⁴⁻³⁵ The atomic relaxations were carried out with a conjugate gradient minimization scheme, until the maximum force on any atom was below 0.01 eV Å⁻¹. The Fermi level was smeared using the Methfessel-Paxton approach³⁶ with a Gaussian width of 0.01 eV, and all energies were extrapolated to T = 0 K. Self-consistency in the electron density was converged up to a precision in the total energy better than 10⁻⁶ eV. On the other hand, the computationally efficient FIREBALL code²⁹⁻³¹ is based on a local-orbital formulation in which self-consistency is implemented on the orbital occupation numbers. The main advantage of using this local-orbital code for our analysis of the PTCDA/TiO₂(110) interface is that it offers an improved description of the electronic structure of organic semiconductor interfaces (in particular, the organic energy gap⁷) due to the inclusion in the code of appropriate corrections, see equations 1 and 2, for the electronic structure calculation. For these local-orbital calculations we have used a basis set of optimized sp^3d^5 numerical atomic orbitals (NAOs)³⁷ for C and Ti, $sp^3s^*p^3*$ for O and s for H, which has been used in previous studies by the authors involving TCNQ and ZnTPP on TiO₂ interfaces, among others (see further details in previous recent literature^{10, 12}). Within the FIREBALL approach we have used the Local Density Approximation (LDA) functional²⁹ and the ion-electron interaction has been modelled by means of norm-conserving scalar-relativistic pseudo-potentials.³⁸

Molecular gap correction and energy alignment approach

Once the optimal ground-state PTCDA/TiO₂ geometries have been established, the organic/oxide interface electronic properties are analysed introducing some corrections within our local-orbital DFT calculations. These corrections are applied to overcome the following well-known limitations of conventional DFT implementations (*e.g.* LDA, GGA): (a) the Kohn-Sham energy levels yield transport gaps for the organic molecules that are usually too small;^{7, 39-40} and (b) the initial relative level alignment between the oxide and the organic materials is poorly described even in well converged LDA (or GGA) calculations.⁴¹⁻⁴⁴ For this purpose, and in accordance with previous publications (see *e.g.* Refs. [10, 12, 39-40, 45]), we have introduced the two following operators to address these problems. With the following scissor operator:

$$O^{scissor} = \sum_{(\mu\nu)} \left\{ \left(\frac{U}{2} \right) |\mu\rangle\langle\mu| - \left(\frac{U}{2} \right) |\nu\rangle\langle\nu| \right\}, \quad (1)$$

$|\mu\rangle$ ($|\nu\rangle$) being the empty (occupied) molecular orbitals of the isolated molecule (with the actual geometry of the molecule on the surface), we open the LDA-energy gap, E_g^{LDA} , to $E_g^{LDA} + U$, where U is fixed to yield the experimental energy gap of 4.1 eV (see below). Additionally, the following shift operator:

$$O^{shift} = \sum_{(\mu\nu)} \{ (\varepsilon) (|\mu\rangle\langle\mu| + |\nu\rangle\langle\nu|) \}, \quad (2)$$

introduces a rigid shift, ε , of the molecular levels; ε is fixed to yield the appropriate *initial* alignment between the oxide and the organic energy levels. These corrections are introduced in the local-orbital Hamiltonian, and the interface electronic structure is then obtained by means of

a self-consistent DFT calculation using the interface atomic geometry obtained with the QUANTUM ESPRESSO code.²⁸

Theoretical STM imaging

Once the electronic structure has been adequately established, theoretical STM calculations have been carried out for all the interfacial configurations considered in this study, to be compared with the experimental images. In order to obtain accurate STM images and tunneling currents, we have used an efficient STM theoretical simulation technique implemented in the FIREBALL code that includes a detailed description of the electronic properties of both the tip and the sample. Using this technique, based on a combination of a Keldysh Green’s function formalism and local orbital density functional theory (DFT),⁴⁶⁻⁴⁸ we split the system into sample and tip, where the samples here are the different systems tested. In these calculations we simulate the scanning with a W-tip formed by 5 atoms (one of them in the apex) attached to an extended W(100)-crystal. Within this approach, in the tunneling regime at low temperature, the STM current is given by:⁴⁶⁻⁴⁸

$$I = \frac{4\pi e^2}{\hbar} \int_{E_F}^{E_F + eV_s} d\omega Tr[T_{ts}\rho_{ss}(\omega)T_{st}\rho_{tt}(\omega - eV)], \tag{3}$$

where V_s is the surface voltage, ρ_{tt} and ρ_{ss} are the density of states (DOS) matrices – in the local orbital basis – associated with the tip and sample, whilst T_{ts} and T_{st} are the local orbital Hamiltonian matrices coupling tip and sample. The overlapping Hamiltonian is obtained by using a dimer approximation: a dimer formed by one W atom (corresponding to the tip) and another (H, C, O and Ti coming from the sample) is calculated for different atom–atom distances and for all the non-zero interactions, using the Keldish-Green formalism to propagate the tunnel current between both subsystems. All the theoretical STM images have been obtained at constant-current scanning conditions, moving the W-tip perpendicularly to the sample in each scanning stage to search a pre-selected fix value of the tunnel current in order to mimic experimental procedure.

III. Results and Discussion

Adsorption geometry

Recent literature investigating the adsorption of the PTCDA molecule or PTCDA-related molecules on the TiO₂(110) surface has produced two geometries as likely candidates for PTCDA adsorption at room temperature. One of the geometries proposed for full monolayer coverage is a flat adsorption mode, with two molecules per unit cell, in which PTCDA binds via its two extreme opposite carboxylic di-anhydride groups to the surface Ti atoms as shown in Figure 1¹⁹⁻²⁰, where details for the molecule located in the unit cell center are shown. We stress that both molecules present very similar adsorption geometries, although the interaction with the substrate is slightly different. The adsorption geometry, resulting in a 18.0 Å x 13.2 Å unit cell, was deduced from a combination of STM measurements and ab-initio calculations including the simulation of STM images in the Tersoff-Hamman approximation. In this geometry, PTCDA is strongly distorted as shown in Figure 1b, with a very large curvature along the small axis. Notice

also that the O-Ti bond lengths are around 2.24 Å, and that the mean distance from the molecule to the surface oxygen layer is 2.37 Å as shown in Figure 1c. These values indicate that there is a strong interaction (and an important charge transfer, as discussed further below) between the molecule and the oxide.

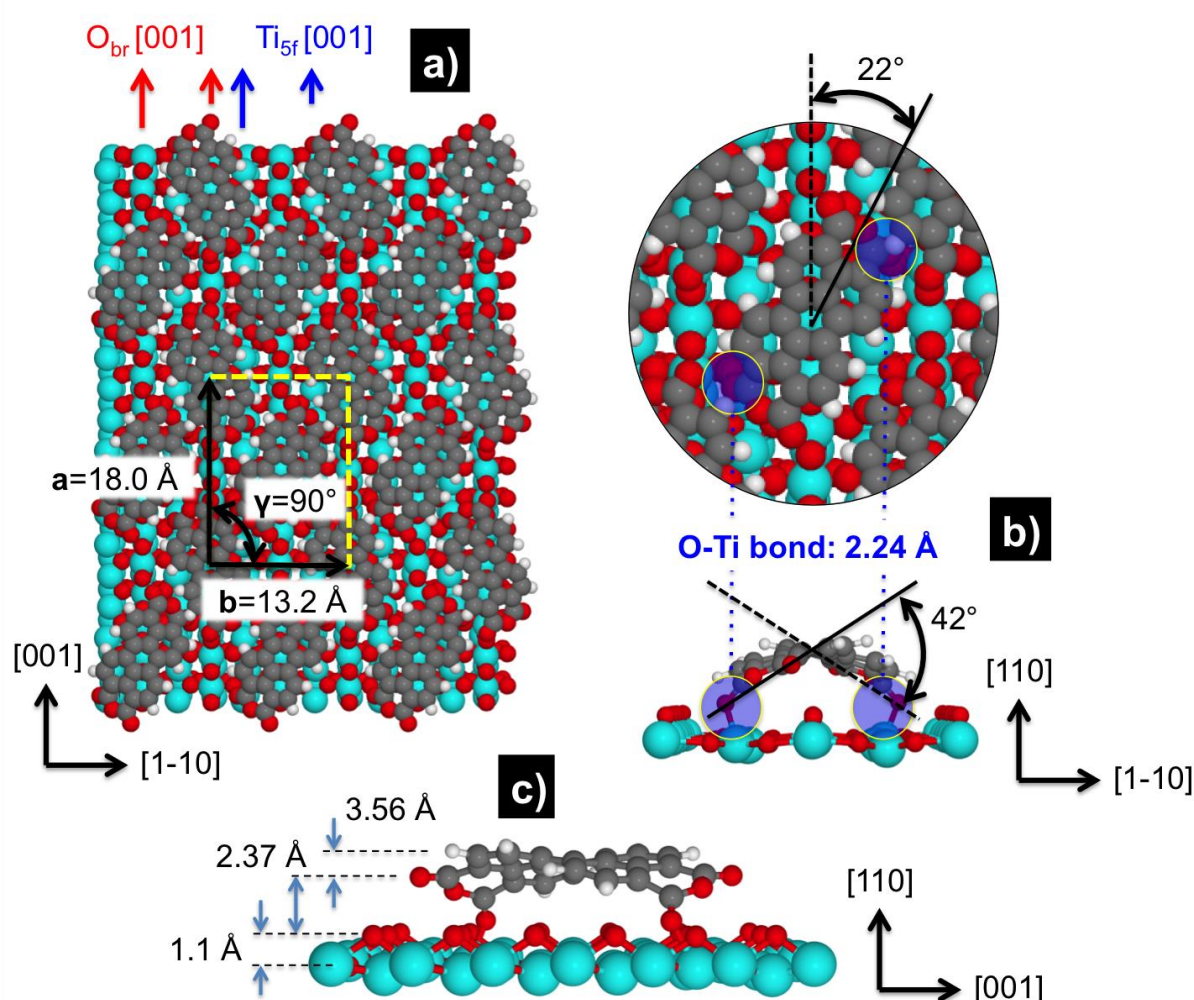


Figure 1: Detailed pictorial views of the optimized geometry corresponding to the optimized flat model: a) Top view indicating the unit cell and the on-surface orientation of the PTCDA molecules; b) Detailed top view (indicating the rotation angle of the longitudinal axis of the PTCDA molecules w.r.t. the TiO_2 O_{br} surface rows) and side view along the main axis showing the distances and torsion angle associated with the molecule curvature; and c) lateral side view showing distances from the molecule to the surface.

In contrast, spectroscopic methods sensitive to the molecular orientation such as NEXAFS indicate that the PTCDA monolayer is most-likely adsorbed in a tilted geometry²⁰⁻²¹. Inspired by recent work on the adsorption of the PTCDI molecule on $\text{TiO}_2(110)$ ²², and on the adsorption of other conjugated planar molecules such as perylene²³ or pentacene²⁴ on $\text{TiO}_2(110)$, we have extrapolated the adsorption geometry found for these molecules to the possible geometry expected for PTCDA: an on-edge geometry, where PTCDA lies along its longer direction and where the PTCDA molecular plane assumes a large tilt angle with respect to the surface as shown in Figure 2. A top view of the resulting system is shown in Figure 2a, along with a side view in Figure 2b. In this configuration the unit cell has $a=b=11.2$ Å, with an angle, γ , between these vectors of 72.5° ; the longer molecular axis is parallel to the $[001]$ direction of the $\text{TiO}_2(110)$ surface, and the tilted angle is 28° (see figure 2). The distance between the molecule Center of Mass (CM) and the oxide oxygen layer is 3.45 Å, much larger than the one found in the flat configuration; this is already an indication of the smaller charge transfer found in tilted case between the molecule and the oxide.

One can in principle compare the adsorption energy of the two different adsorption modes in order to determine the favored model. However, in our case, the total energy calculations using the Quantum Espresso code for the tilted and the flat molecules on the oxide surface have yielded energy differences between the two cases smaller than 50 meV per molecule; this is too small to be used as a way of discarding one of the two models. Consequently, we have used other data, STM-images and interface dipoles to discriminate between the two models.

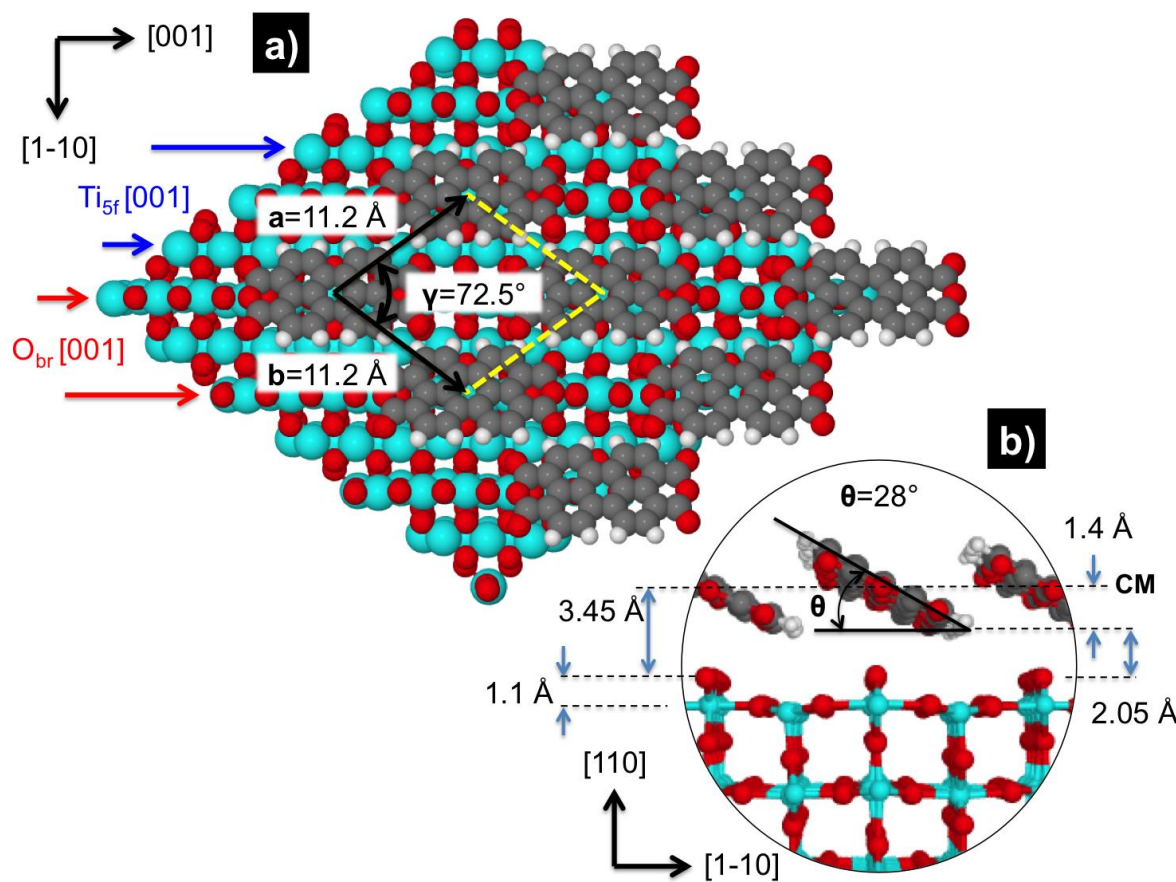


Figure 2: Detailed pictorial views of the optimized geometry corresponding to the tilted model: a) Top view indicating the resulting unit cell and the on-surface orientation of the PTCDA molecules; and b) Side view showing distances from the molecule to the surface and the tilt angle (CM stands for the molecule Center of Mass).

In order to compare our results to existing STM images for PTCDA adsorbed on the $\text{TiO}_2(110)$ surface, we have simulated the STM images corresponding to each adsorption mode using a combination of a Green's function formalism and local-orbital DFT, as described in section II. Figure 3 presents the calculated images obtained for both geometries for a tunneling bias of $V_s=+2.0$ V and an intensity of 1 nA. For simplicity, the details of the corrections introduced in the local-orbital DFT electronic structure calculation (equations 1 and 2) are discussed in the next section, although the corrections to the energy alignment are taken into account in these images. The image for the tilted geometry captures the side of the molecule protruding from the surface. The image for the flat geometry, that reflects the upper part of the molecules, shows that the two molecules per unit cell have a similar morphology but exhibit a slightly different contrast due to their different interaction with the substrate.

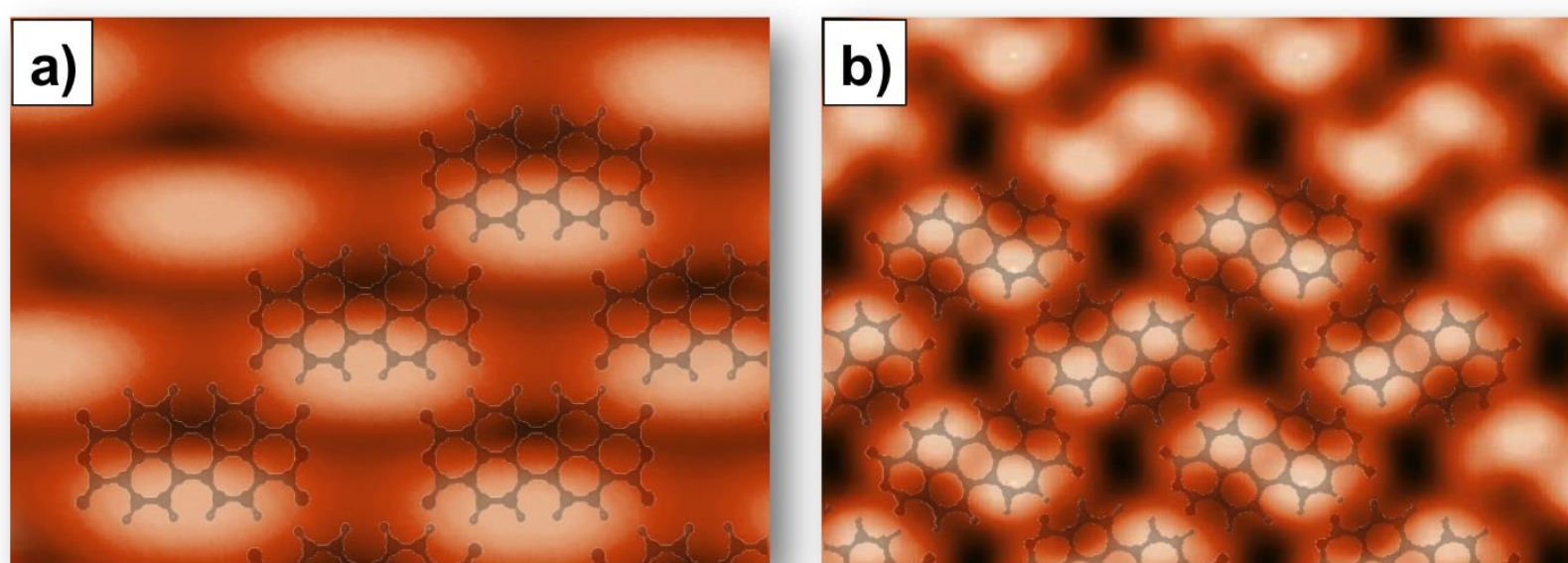


Figure 3: Theoretical STM images obtained for a) the tilted and b) the flat adsorption geometries.

Theoretical images for the tilted model are very close to the experimental ones¹⁹, while the images for the flat model show a different picture; so, the present STM calculations favor the tilted structure. We should say that in Godlewski et al's calculations¹⁹, the theoretical STM image is much closer to the experimental one. We believe that this is due to the Tersoff-Hamann's approximation used to calculate the tunneling currents in this earlier work: the method we have used in our approach is much more accurate since it includes all the tip electronic structure and its interaction with the molecule⁴⁶⁻⁴⁸.

Energy alignment and electronic structure

We now switch to the problem of energy alignment at the interface between PTCDA and TiO₂(110). Figure 4 shows the Ti 2p, O 1s and C 1s core levels spectra measured using XPS on the TiO₂(110) surface before (black), after deposition of 1ML of PTCDA (green) and after deposition of a thick multilayer of PTCDA (ochre). Both before and after deposition of a monolayer of PTCDA, the binding energies of the Ti 2p (found at -458.7 eV and -464.3 eV) and the O 1s (found at -529.8 eV) core levels of the substrate are unchanged indicating no band bending is induced by the molecular adsorption. In the monolayer regime, the O 1s spectrum is still dominated by the oxide core level of the substrate, and only a small shoulder is visible near a binding energy of -532 eV. However, the C 1s spectrum indicates the presence of PTCDA, with its two characteristic peaks found at -285.1 eV and -289.2 eV, corresponding to the perylene core and to the dianhydride carboxylic groups of the molecule, respectively. For the multilayer, the PTCDA core levels contribution is increased, as expected.

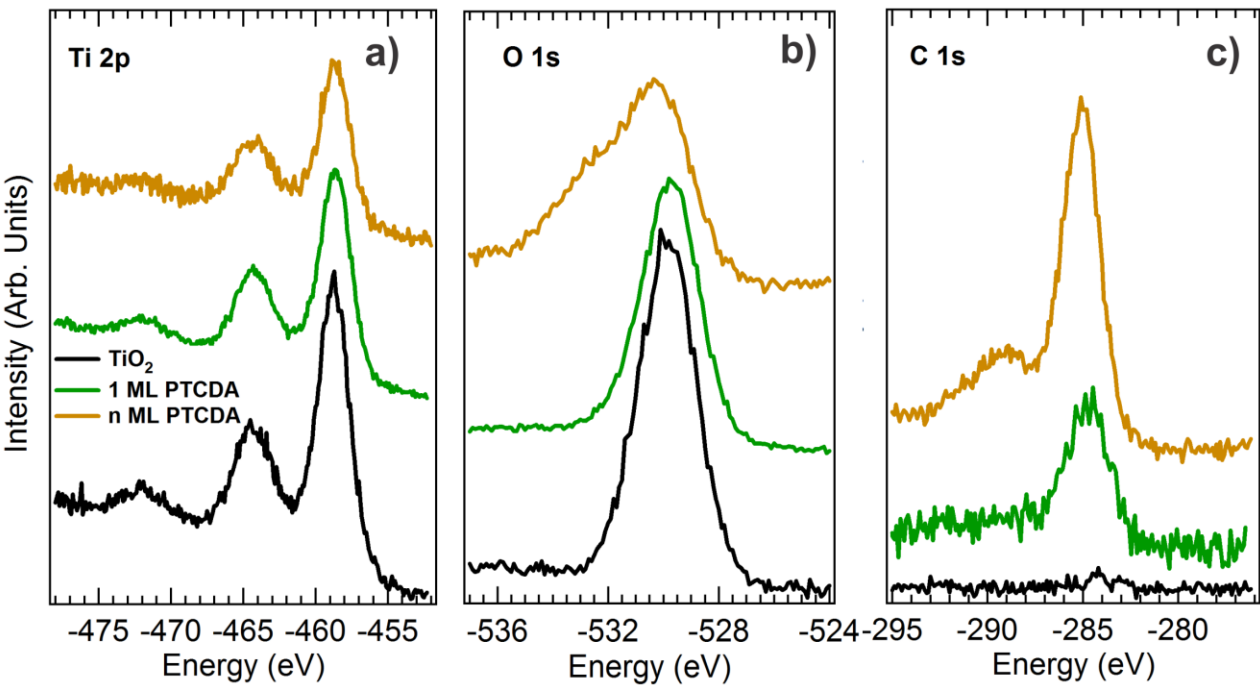


Figure 4: a) Ti 2p, b) O 1s and c) C 1s core level spectra measured on clean the TiO₂(110) surface (black), after deposition of one monolayer of PTCDA (green) and after deposition of a thick multilayer (ochre).

Figure 5 displays the secondary electron cutoffs obtained from UPS (Figure 5a), as well as the VB and CB spectra measured using UPS and IPS for a multilayer (Figure 5b) and a monolayer (Figure 5c) of PTCDA on TiO₂(110). The energy scale is referenced to the measured Fermi level of the system set at 0, so that occupied states occur at negative energies and unoccupied states occur at positive energies. These spectra were measured on the TiO₂(110) surface before and after deposition of 1 ML of PTCDA (Figure 5c) and after subsequent deposition of a thick PTCDA multilayer (Figure 5b).

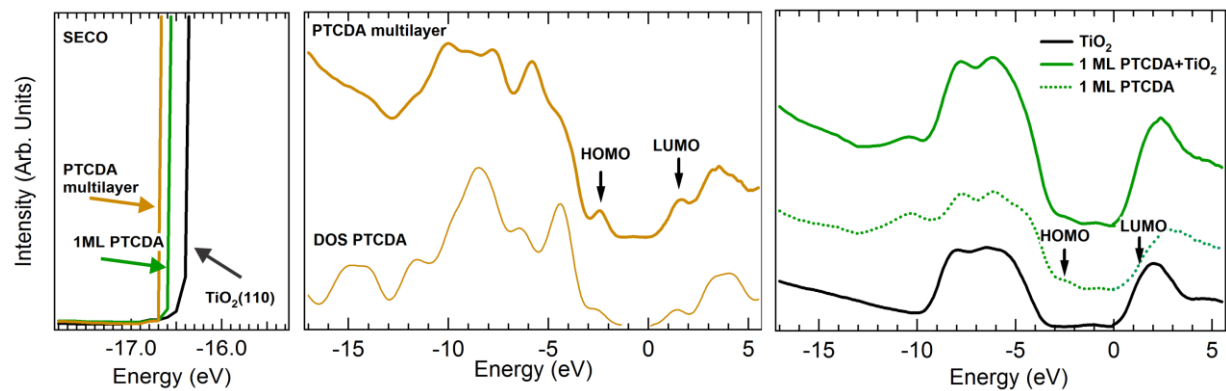


Figure 5: a) SECO measured on the clean TiO₂(110) surface, and after deposition of 1ML and of a thick multilayer. b) VB and CB measured on a thick PTCDA multilayer compared to the DOS calculated for a PTCDA molecule. c) VB and CB of the TiO₂(110) surface before (black) and after deposition of 1ML PTCDA (solid green). The experimental position of the HOMO and LUMO are indicated on the PTCDA spectral counterpart of the monolayer (dotted green).

It is usually easier to interpret the electronic structure of multilayers as they resemble the electronic structure of individual molecules. Figure 5b presents the VB and CB spectra measured (bold curve) on a multilayer thick enough to neglect the substrate contribution at these energies, compared to the density of states (DOS) calculated (thin curve) for the PTCDA molecule (GAMESS US⁴⁹, B3LYP⁵⁰⁻⁵², 6-31G*⁵³) and adjusted to fit the experimental HOMO-LUMO gap. Although cross section effects are not taken into account in the calculated DOS, the

experimental features in both occupied and unoccupied states are well described by the DOS. The centroids of the HOMO and LUMO are therefore found at -2.5 eV and 1.6 eV, respectively, leading to an energy gap of 4.1 eV. The electron affinity of the multilayer can be calculated from both the position of the SECO measured on the thick film (shown in Figure 5a) and from the measured HOMO-LUMO gap, which gives a value of 3 eV.

Before analyzing the monolayer coverage of PTCDA, it is important to consider the clean TiO_2 substrate properties. The VB and CB measured on the clean surface, shown as the black curve in Figure 5c, are characteristic of the nearly stoichiometric $\text{TiO}_2(110)$ surface: the VB is comprised mostly of O 2p states and spans the energy range from -10 eV to -3 eV and, depending on the surface preparation, Ti^{3+} defect states of weak intensity can be found around -1 eV. The CB is characterized by strong emission associated with empty Ti 3d states found between 0 and 4 eV. A linear extrapolation of the valence and conduction band edges to the spectra background leads to a valence band maximum and a conduction band minimum at -3.4 eV and 0.2 eV, respectively and thus to a gap of 3.6 eV, similar to previously reported values.^{10, 12, 27, 54} Using the SECO measured on the clean surface reported in Figure 5a, the electron affinity of the clean surface is found to be 4.6 eV. Upon deposition of a monolayer of PTCDA, molecular features are apparent on both the occupied and unoccupied states, shown as continuous green curves in Figure 5c. As these spectra contain contributions from both the monolayer and the TiO_2 substrate, and as no band bending occurs upon PTCDA deposition, subtracting the substrate contribution is straightforward and the resulting molecular contribution of the adsorbed PTCDA monolayer is shown as a green dotted line in Figure 5c. The frontier orbitals of the adsorbed monolayer are broader than those of the multilayer, but one can still evaluate their positions: within our error bars, they are found identical to the one measured for the multilayer. This is in accordance with the work of Cao et al.²¹ Finally, the electron affinity measured for the PTCDA monolayer is 0.2 eV larger than the one measured for the PTCDA multilayer. The resulting set of data can be represented as an energy diagram as shown in Figure 6a, and emphasizes the presence of an interfacial dipole of 0.3 eV developing upon deposition of the PTCDA monolayer on $\text{TiO}_2(110)$. The overall energy alignment measured here is in qualitative agreement with previous reports.²¹

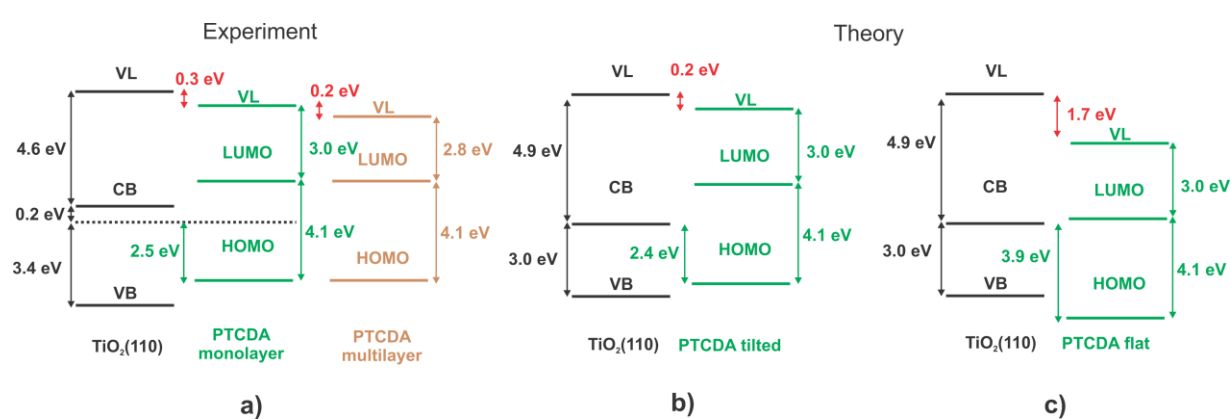


Figure 6: a) Experimental energy diagrams for a 1ML PTCDA and for a multilayer adsorbed on $\text{TiO}_2(110)$, compared to the theoretical energy alignment calculated for b) the tilted geometry and for c) the flat geometry.

In parallel, we have analyzed theoretically the interface energy level alignment by means of a local-orbital DFT code (FIREBALL), using the geometries provided by a plane-wave DFT code

(QUANTUM ESPRESSO). We have considered the two adsorption geometries proposed in Figures 1 and 2 for PTCDA.

As presented above, both a shift operator ϵ and a scissor operator U have been introduced into our local-orbital Hamiltonian, in order to initially reproduce the LUMO and HOMO experimental values measured for the PTCDA monolayer shown in Figure 6a. For both adsorbed geometries, the corrected HOMO-LUMO gap was fixed to 4.1 eV, and the molecule electron affinity to 3.0 eV. Notice also that in our calculations the TiO_2 -energy gap, 3.0 eV, is a little smaller than the experimental one, 3.6 eV; in our calculations we have minimized the errors associated with this theoretical gap, by increasing our theoretical oxide affinity by 0.3 eV (see Figures 6b and c), so that the mid-gap position coincides with the experimental one. The final energy alignment obtained for the two different adsorption modes is shown in Figure 6b and Figure 6c for the tilted and flat geometries, respectively. The corresponding partial DOS, projected on the TiO_2 substrate and on the PTCDA molecules are shown in Figure 7a and Figure 7b for the tilted and flat geometries, respectively.

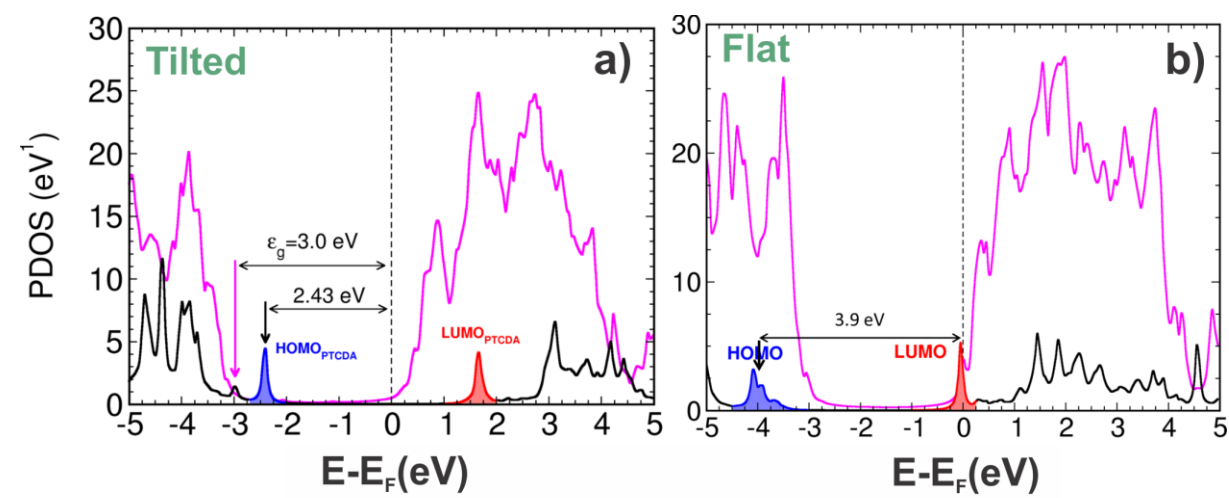


Figure 7: Partial DOS projected on TiO_2 and on PTCDA highlighting the positions of the HOMO and LUMO levels for a) the tilted geometry and b) the flat geometry.

The major difference highlighted by the calculations is the presence of a large interface dipole of 1.7 eV obtained in the case of the flat adsorption geometry, much larger than the 0.2 eV interface dipole yielded by the titled geometry. This large interface dipole has two main sources: a 0.35 electrons/molecule charge transfer from the PTCDA molecule to the TiO_2 surface arising from the strong bonding of the molecule to the surface in this geometry and leading to an interface dipole of 1.1 eV, as well as a purely molecular dipole associated with the important deformation of the PTCDA molecule and calculated to be 0.6 eV. In this geometry, the PTCDA HOMO centroid is found deep into the TiO_2 VB, 3.9 eV below the CB minimum. The small interface dipole calculated for the tilted geometry is due to the small amount of charge transferred from the molecule to the oxide, around 0.07 electrons/molecule. Thus this geometry yields an interface dipole in excellent agreement with the experimental data of Figure 6a. Moreover, in the case of the tilted model, the HOMO level is inside the TiO_2 gap, while the LUMO level is well inside the TiO_2 conduction band, in good agreement with the experimental evidence (Fig. 5c). Therefore, both from STM images simulations and from the expected effect

of the adsorption geometry of PTCDA on $\text{TiO}_2(110)$ on the energy alignment at the interface, the titled geometry for PTCDA at the monolayer regime appears as the most-likely candidate.

Based on the recent literature addressing the interface between organic molecules and $\text{TiO}_2(110)$,^{10, 12} a set of general comments can be made. First, at the surface of $\text{TiO}_2(110)$, strong bonding can occur and leads to important intramolecular distortion as well as to significant charge transfer between the organic layer and the surface.^{10, 12} In particular, at room temperature charge transfer can result in band bending into the $\text{TiO}_2(110)$ substrate.¹⁰ Moreover, molecule-molecule interactions can lead to an alteration of the geometry expected for a molecule isolated on the surface, thereby altering charge transfer and consequently the interface dipole.¹² The energy alignment at the surface of $\text{TiO}_2(110)$ appears as a multifaceted problem for which individual cases should be carefully studied. The energy alignment for PTCDA on $\text{TiO}_2(110)$ is not an exception to this observation. For example, although PTCDA has a large electron affinity, comparable to the well-studied TCNQ (tetracyanoquinodimethane) molecule, its energy alignment does not result in a behavior that is similar to TCNQ on $\text{TiO}_2(110)$. In the case of TCNQ, the molecule forms a strong chemical bond with the surface resulting in substantial charge transfer that gives rise to a large interface dipole and band bending in the substrate.¹⁰ For PCTDA, a titled geometry is favored at the surface of $\text{TiO}_2(110)$ leading to a weak interface dipole. As such, general rules for the precise prediction of the energy alignment at the oxide-organic interface seem difficult to establish.

IV. Conclusion

The occupied and unoccupied electronic structures of the PTCDA molecule adsorbed on the $\text{TiO}_2(110)$ surface has been determined experimentally using XPS, UPS and IPS, in order to establish a detailed energy alignment description of the interface. In parallel, two possible geometries, flat or tilted, proposed in the literature for the adsorption of PTCDA on $\text{TiO}_2(110)$ have been explored using DFT, and paying especial attention to the interface energy level alignment and to theoretical STM images.

Contrary to previous reports, both STM images simulation and resulting energy alignment point to a titled geometry for PTCDA on $\text{TiO}_2(110)$. The detailed treatment of the STM simulation undertaken in this work, as compared to a simpler Tersoff-Hamman approach, could reproduce the existing experimental STM data using a titled geometry. Additionally, in a flat geometry, strong molecular distortion and charge transfer from the molecule to the substrate take place, and lead to a large interface dipole of 1.7 eV, incompatible with our experimental energy alignment. In the tilted geometry, weaker charge transfer is calculated with little molecular alteration, leading to a smaller interface dipole of 0.2 eV, in excellent agreement with the experimental value of 0.3 eV.

AUTHOR INFORMATION

Corresponding Author: Fernando Flores

*E-mail: fernando.flores@uam.es ; rangan@physics.rutgers.edu

*Phones : 34-91-4975043; 848-445-8419

Notes

The authors declare no competing financial interests.

ACKNOWLEDGMENT

SR, CR, and RAB acknowledge support from the Department of Energy under Grant No FG02-01ER15256. CR acknowledges support from the Peter Lindenfeld Graduate Fellowship. JIM acknowledges funding from the ERC-Synergy Program (Grant ERC-2013-SYG-610256 NANOCOSMOS). FF and JO acknowledge support from the Spanish Ministerio de Economía y Competitividad (MINECO) under project MAT2014-59966-R and through the “María de Maeztu” Program for Units of Excellence in R&D (MDM-2014-0377)”

REFERENCES

1. Forrest, S. R. Ultrathin Organic Films Grown by Organic Molecular Beam Deposition and Related Techniques. *Chem Rev* **1997**, *97*, 1793-1896.
2. Kabra, D.; Lu, L. P.; Song, M. H.; Snaith, H. J.; Friend, R. H. Efficient Single-Layer Polymer Light-Emitting Diodes. *Adv. Mater.* **2010**, *22*, 3194-+.
3. Li, H.; Winget, P.; Brédas, J.-L. Transparent Conducting Oxides of Relevance to Organic Electronics: Electronic Structures of Their Interfaces with Organic Layers. *Chemistry of Materials* **2014**, *26*, 631-646.
4. Meyer, J.; Hamwi, S.; Kroger, M.; Kowalsky, W.; Riedl, T.; Kahn, A. Transition Metal Oxides for Organic Electronics: Energetics, Device Physics and Applications. *Adv. Mater.* **2012**, *24*, 5408-5427.
5. Sessolo, M.; Bolink, H. J. Hybrid Organic-Inorganic Light-Emitting Diodes. *Adv. Mater.* **2011**, *23*, 1829-1845.
6. Cahen, D.; Kahn, A.; Umbach, E. Energetics of Molecular Interfaces. *Mater Today* **2005**, *8*, 32-41.
7. Flores, F.; Ortega, J.; Vazquez, H. Modelling Energy Level Alignment at Organic Interfaces and Density Functional Theory. *Phys Chem Chem Phys* **2009**, *11*, 8658-8675.
8. Koch, N. Energy Levels at Interfaces between Metals and Conjugated Organic Molecules. *Journal of Physics: Condensed Matter* **2008**, *20*, 184008.
9. Greiner, M. T.; Helander, M. G.; Tang, W.-M.; Wang, Z.-B.; Qiu, J.; Lu, Z.-H. Universal Energy-Level Alignment of Molecules on Metal Oxides. *Nat Mater* **2012**, *11*, 76-81.
10. Martínez, J. I.; Flores, F.; Ortega, J.; Rangan, S.; Ruggieri, C.; Bartynski, R. Chemical Interaction, Space-Charge Layer, and Molecule Charging Energy for a Tio2/Tcnq Interface. *The Journal of Physical Chemistry C* **2015**, *119*, 22086-22091.
11. Xu, Y., et al. Space-Charge Transfer in Hybrid Inorganic-Organic Systems. *Phys. Rev. Lett.* **2013**, *111*.
12. Rangan, S.; Ruggieri, C.; Bartynski, R.; Martínez, J. I.; Flores, F.; Ortega, J. Densely Packed Zntpps Monolayer on the Rutile Tio2(110)-(1 × 1) Surface: Adsorption Behavior and Energy Level Alignment. *The Journal of Physical Chemistry C* **2016**, *120*, 4430-4437.
13. Winget, P., et al. Defect-Driven Interfacial Electronic Structures at an Organic/Metal-Oxide Semiconductor Heterojunction. *Adv. Mater.* **2014**, *26*, 4711-+.
14. Tautz, F. S. Structure and Bonding of Large Aromatic Molecules on Noble Metal Surfaces: The Example of Ptcda. *Prog Surf Sci* **2007**, *82*, 479-520.
15. Proehl, H.; Dienel, T.; Nitsche, R.; Fritz, T. Formation of Solid-State Excitons in Ultrathin Crystalline Films of Ptcda: From Single Molecules to Molecular Stacks. *Phys. Rev. Lett.* **2004**, *93*.
16. Yamane, H.; Kera, S.; Okudaira, K. K.; Yoshimura, D.; Seki, K.; Ueno, N. Intermolecular Energy-Band Dispersion in Ptcda Multilayers. *Phys Rev B* **2003**, *68*.
17. Chen, W.; Huang, H.; Chen, S.; Chen, L.; Zhang, H. L.; Gao, X. Y.; Wee, A. T. S. Molecular Orientation of 3,4,9,10-Perylene-Tetracarboxylic-Dianhydride Thin Films at Organic Heterojunction Interfaces. *Appl. Phys. Lett.* **2007**, *91*.
18. Martínez, J. I.; Abad, E.; Flores, F.; Ortega, J.; Brocks, G. Barrier Height Formation for the Ptcda/Au(1 1 1) Interface. *Chem. Phys.* **2011**, *390*, 14-19.
19. Godlewski, S.; Prauzner-Bechcicki, J. S.; Glatzel, T.; Meyer, E.; Szymonski, M. Transformations of Ptcda Structures on Rutile Tio2 Induced by Thermal Annealing and Intermolecular Forces. *Beilstein J Nanotech* **2015**, *6*, 1498-1507.

20. Godlewski, S.; Tekiel, A.; Piskorz, W.; Zasada, F.; Prauzner-Bechcicki, J. S.; Sojka, Z.; Szymonski, M. Supramolecular Ordering of Ptcda Molecules: The Key Role of Dispersion Forces in an Unusual Transition from Physisorbed into Chemisorbed State. *Acs Nano* **2012**, *6*, 8536-8545.
21. Cao, L.; Wang, Y. Z.; Zhong, J. Q.; Han, Y. Y.; Zhang, W. H.; Yu, X. J.; Xu, F. Q.; Qi, D. C.; Wee, A. T. S. Electronic Structure, Chemical Interactions and Molecular Orientations of 3,4,9,10-Perylene-Tetracarboxylic-Dianhydride on Tio2(110). *J Phys Chem C* **2011**, *115*, 24880-24887.
22. Cao, L.; Wang, Y. Z.; Zhong, J. Q.; Han, Y. Y.; Zhang, W. H.; Yu, X. J.; Xu, F. Q.; Qi, D. C.; Wee, A. T. S. Molecular Orientation and Site Dependent Charge Transfer Dynamics at Ptcda/Tio2(110) Interface Revealed by Resonant Photoemission Spectroscopy. *J Phys Chem C* **2014**, *118*, 4160-4166.
23. Lanzilotto, V.; Lovat, G.; Otero, G.; Sanchez, L.; Lopez, M. F.; Mendez, J.; Martin-Gago, J. A.; Bavdek, G.; Floreano, L. Commensurate Growth of Densely Packed Ptcdi Islands on the Rutile Tio2(110) Surface. *J Phys Chem C* **2013**, *117*, 12639-12647.
24. Otero-Irurueta, G.; Martinez, J. I.; Lovat, G.; Lanzilotto, V.; Mendez, J.; Lopez, M. F.; Floreano, L.; Martin-Gago, J. A. Densely Packed Perylene Layers on the Rutile Tio2(110)-(1 X 1) Surface. *J Phys Chem C* **2015**, *119*, 7809-7816.
25. Lanzilotto, V.; Sanchez-Sanchez, C.; Bavdek, G.; Cvetko, D.; Lopez, M. F.; Martin-Gago, J. A.; Floreano, L. Planar Growth of Pentacene on the Dielectric Tio2(110) Surface. *J Phys Chem C* **2011**, *115*, 4664-4672.
26. Komolov, A. S.; Moller, P. J.; Mortensen, J.; Komolov, S. A.; Lazneva, E. F. Modification of the Electronic Properties of the Tio2 (110) Surface Upon Deposition of the Ultrathin Conjugated Organic Layers. *Appl. Surf. Sci.* **2007**, *253*, 7376-7380.
27. Rangan, S.; Katalinic, S.; Thorpe, R.; Bartynski, R. A.; Rochford, J.; Galoppini, E. Energy Level Alignment of a Zinc(Ii) Tetraphenylporphyrin Dye Adsorbed onto Tio2(110) and Zno(11(2)over-Bar0) Surfaces. *J Phys Chem C* **2010**, *114*, 1139-1147.
28. Giannozzi, P., et al. Quantum Espresso: A Modular and Open-Source Software Project for Quantum Simulations of Materials. *J Phys-Condens Mat* **2009**, *21*.
29. Jelinek, P.; Wang, H.; Lewis, J. P.; Sankey, O. F.; Ortega, J. Multicenter Approach to the Exchange-Correlation Interactions in Ab Initio Tight-Binding Methods. *Phys Rev B* **2005**, *71*.
30. Lewis, J. P.; Glaesemann, K. R.; Voth, G. A.; Fritsch, J.; Demkov, A. A.; Ortega, J.; Sankey, O. F. Further Developments in the Local-Orbital Density-Functional-Theory Tight-Binding Method. *Phys Rev B* **2001**, *64*.
31. Lewis, J. P.; Jelinek, P.; Ortega, J.; Demkov, A. A.; Trabada, D. G.; Haycock, B.; Wang, H.; Adams, G.; Tomfohr, J. K.; Abad, E. Advances and Applications in the Fireballab Initio Tight-Binding Molecular-Dynamics Formalism. *physica status solidi (b)* **2011**, *248*, 1989-2007.
32. Perdew, J. P.; Burke, K.; Ernzerhof, M. Generalized Gradient Approximation Made Simple (Vol 77, Pg 3865, 1996). *Phys. Rev. Lett.* **1997**, *78*, 1396-1396.
33. Monkhorst, H. J.; Pack, J. D. Special Points for Brillouin-Zone Integrations. *Phys Rev B* **1976**, *13*, 5188-5192.
34. Barone, V.; Casarin, M.; Forrer, D.; Pavone, M.; Sami, M.; Vittadini, A. Role and Effective Treatment of Dispersive Forces in Materials: Polyethylene and Graphite Crystals as Test Cases. *J Comput Chem* **2009**, *30*, 934-939.
35. Grimme, S. Semiempirical Gga-Type Density Functional Constructed with a Long-Range Dispersion Correction. *J Comput Chem* **2006**, *27*, 1787-1799.
36. Methfessel, M.; Paxton, A. T. High-Precision Sampling for Brillouin-Zone Integration in Metals. *Phys Rev B* **1989**, *40*, 3616-3621.
37. Basanta, M. A.; Dappe, Y. J.; Jelinek, P.; Ortega, J. Optimized Atomic-Like Orbitals for First-Principles Tight-Binding Molecular Dynamics. *Comp Mater Sci* **2007**, *39*, 759-766.
38. Fuchs, M.; Scheffler, M. Ab Initio Pseudopotentials for Electronic Structure Calculations of Poly-Atomic Systems Using Density-Functional Theory. *Comput Phys Commun* **1999**, *119*, 67-98.
39. Beltran, J. I.; Flores, F.; Martinez, J. I.; Ortega, J. Energy Level Alignment in Organic-Organic Heterojunctions: The Ttf/Tcnq Interface. *J Phys Chem C* **2013**, *117*, 3888-3894.
40. Martinez, J. I.; Abad, E.; Beltran, J. I.; Flores, F.; Ortega, J. Barrier Height Formation in Organic Blends/Metal Interfaces: Case of Tetrathiafulvalene-Tetracyanoquinodimethane/Au(111). *J Chem Phys* **2013**, *139*.
41. Biller, A.; Tamblyn, I.; Neaton, J. B.; Kronik, L. Electronic Level Alignment at a Metal-Molecule Interface from a Short-Range Hybrid Functional. *J Chem Phys* **2011**, *135*.
42. Chen, W.; Tegenkamp, C.; Pfnur, H.; Bredow, T. Anomalous Molecular Orbital Variation Upon Adsorption on a Wide Band Gap Insulator. *J Chem Phys* **2010**, *132*.
43. Freysoldt, C.; Rinke, P.; Scheffler, M. Controlling Polarization at Insulating Surfaces: Quasiparticle Calculations for Molecules Adsorbed on Insulator Films. *Phys. Rev. Lett.* **2009**, *103*.
44. Kronik, L.; Fromherz, R.; Ko, E.; Gantefor, G.; Chelikowsky, J. R. Photoemission Spectra of Deuterated Silicon Clusters: Experiment and Theory. *Eur Phys J D* **2003**, *24*, 33-36.
45. Abad, E.; Dappe, Y. J.; Martinez, J. I.; Flores, F.; Ortega, J. C6h6/Au(111): Interface Dipoles, Band Alignment, Charging Energy, and Van Der Waals Interaction. *J Chem Phys* **2011**, *134*.
46. Blanco, J. M.; Flores, F.; Perez, R. Stm-Theory: Image Potential, Chemistry and Surface Relaxation. *Prog Surf Sci* **2006**, *81*, 403-443.
47. Blanco, J. M.; Gonzalez, C.; Jelinek, P.; Ortega, J.; Flores, F.; Perez, R. First-Principles Simulations of Stm Images: From Tunneling to the Contact Regime. *Phys Rev B* **2004**, *70*.
48. Gonzalez, C.; Snijders, P. C.; Ortega, J.; Perez, R.; Flores, F.; Rogge, S.; Weitering, H. H. Formation of Atom Wires on Vicinal Silicon. *Phys. Rev. Lett.* **2004**, *93*.
49. Schmidt, M. W., et al. General Atomic and Molecular Electronic-Structure System. *J Comput Chem* **1993**, *14*, 1347-1363.
50. Becke, A. D. Density-Functional Exchange-Energy Approximation with Correct Asymptotic-Behavior. *Phys Rev A* **1988**, *38*, 3098-3100.
51. Becke, A. D. Density-Functional Thermochemistry .3. The Role of Exact Exchange. *J Chem Phys* **1993**, *98*, 5648-5652.

52. Lee, C. T.; Yang, W. T.; Parr, R. G. Development of the Colle-Salvetti Correlation-Energy Formula into a Functional of the Electron-Density. *Phys Rev B* **1988**, *37*, 785-789.

53. Schuchardt, K. L.; Didier, B. T.; Elsethagen, T.; Sun, L. S.; Gurumoorthi, V.; Chase, J.; Li, J.; Windus, T. L. Basis Set Exchange: A Community Database for Computational Sciences. *J Chem Inf Model* **2007**, *47*, 1045-1052.

54. Rangan, S.; Coh, S.; Bartynski, R. A.; Chitre, K. P.; Galoppini, E.; Jaye, C.; Fischer, D. Energy Alignment, Molecular Packing, and Electronic Pathways: Zinc(Ii) Tetraphenylporphyrin Derivatives Adsorbed on Tio2(110) and Zno(11-20) Surfaces. *J Phys Chem C* **2012**, *116*, 23921-23930.

TOC graphic

